


COMMUNICATION

Anatomical variants identified on chest computed tomography of 1000+ COVID-19 patients from an open-access dataset

Laphatrada Yurasakpong^{1,2}  | Somluk Asuvapongpatana¹  |
 Wattana Weerachayanukul¹  | Krai Meemon¹  | Nopporn Jongkamonwiwat¹  |
 Nutmethee Kruepunga^{1,2}  | Arada Chaiyamon³  | Thanwa Sudsang⁴ |
 Joe Iwanaga^{5,6,7,8}  | R. Shane Tubbs^{5,9,10,11}  | Athikhun Suwannakhan^{1,2} 

¹Department of Anatomy, Faculty of Science, Mahidol University, Bangkok, Thailand

²In Silico and Clinical Anatomy Research Group (iSCAN), Bangkok, Thailand

³Department of Anatomy, Faculty of Medicine, Khon Kaen University, KhonKaen, Thailand

⁴Department of Diagnostic and Therapeutic Radiology, Faculty of Medicine Ramathibodi Hospital, Mahidol University, Bangkok, Thailand

⁵Department of Neurosurgery, Tulane University School of Medicine, Louisiana, USA

⁶Department of Neurology, Tulane University School of Medicine, New Orleans, LA, USA

⁷Dental and Oral Medical Center, Kurume University School of Medicine, Fukuoka, Japan

⁸Department of Anatomy, Kurume University School of Medicine, Fukuoka, Japan

⁹Department of Structural and Cellular Biology, Tulane University School of Medicine, New Orleans, LA, USA

¹⁰Department of Neurosurgery, Ochsner Neuroscience Institute, Ochsner Health System, New Orleans, LA, USA

¹¹Department of Anatomical Sciences, St. George's University, St. George's, Grenada

Correspondence

Athikhun Suwannakhan, Department of Anatomy, Faculty of Science, Mahidol University, Rama VI Road, Ratchathewi, Bangkok, 10400 Thailand.
 Email: athikhun.suw@mahidol.edu

Funding information

Faculty of Science, Mahidol University, Grant/Award Number: -

Abstract

Chest computed tomography (CT) has been the preferred imaging modality during the pandemic owing to its sensitivity in detecting COVID-19 infections. Recently, a large number of COVID-19 imaging datasets have been deposited in public databases, leading to rapid advances in COVID-19 research. However, the application of these datasets beyond COVID-19-related research has been little explored. The authors believe that they could be used in anatomical research to elucidate the link between anatomy and disease and to study disease-related alterations to normal anatomy. Therefore, the present study was designed to investigate the prevalence of six well-known anatomical variants in the thorax using open-access CT images obtained from over 1000 Iranian COVID-19 patients aged between 6 and 89 years (60.9% male and 39.1% female). In brief, we found that the azygos lobe, tracheal bronchus, and cardiac bronchus were present in 0.8%, 0.2%, and 0% of the patients, respectively. Variations of the sternum, including sternal foramen, episternal ossicles, and sternalis muscle, were observed in 9.6%, 2.9%, and 1.5%, respectively. We believe anatomists could benefit from using open-access datasets as raw materials for research because these datasets are freely accessible and are abundant, though further research is needed to evaluate the uses of other datasets from different body regions and imaging modalities. Radiologists should also be aware of these common anatomical variants when examining lung CTs, especially since the use of this imaging modality has increased during the pandemic.

KEYWORDS

bronchi, computed tomography, COVID-19, dataset, lung, trachea

1 | INTRODUCTION

During the ongoing COVID-19 pandemic, chest CT has become the preferred imaging modality in clinically suspected patients owing to its high sensitivity (Khatami et al., 2020) and its ability to discriminate between COVID-19 and other pathologies (Azadbakht et al., 2020). Chest CT is also easy to perform and allows sufficiently quick diagnoses for effective therapeutic decisions to be made early in the disease progression (Salahshour et al., 2021). In addition, CT imaging provides information on disease severity and is useful for monitoring patients during treatment and recovery (Tang et al., 2021). Because of these advantages, it is currently being used for diagnosis, screening, and management of COVID-19 worldwide. This has led to a requirement for many scans, keeping radiologists occupied, and has had an unprecedented influence on the radiology training (Fossey et al., 2021). Coupled with limited access to well-trained radiologists with adequate expertise in some regions of the world, there is a call for automation as an alternative approach to detecting COVID-19. Recent studies have employed a data-driven and artificial intelligence approach for automatic detection of COVID-19 based on CT images. This approach requires a large-scale supply of heterogeneous CT images for better performance and accuracy. As a result, a substantial number of COVID-19 imaging datasets have been uploaded to online depositories and have become freely accessible (Afshar et al., 2021; Harmon et al., 2020; Shakouri et al., 2021). This has demonstrably led to new advances in COVID-19-related research.

Despite the usefulness of open-access CT datasets for image recognition and artificial intelligence (AI)-assisted diagnosis, the applications of these datasets beyond COVID-19-related research have been little explored. Anatomical variations are not uncommon in chest CTs (Duraikannu et al., 2016). By comparing the prevalences of such variants between healthy individuals and COVID-19 patients, a plausible relationship between anatomy and disease could be elucidated. Such a comparison could also help to determine whether anatomical variants influence predisposition to COVID-19 infection, and to examine any changes to normal anatomy induced by the disease. In addition, the vast number of public datasets made public since the beginning of the pandemic (Harmon et al., 2020; Santosh & Ghosh, 2021; Wang et al., 2021) could be re-purposed for other types of research not directly relevant to COVID-19. Understanding of these anatomical variants is also crucial for radiologists to avoid misdiagnosis, particularly at the present time when the use of chest CT has increased rapidly. Therefore, this study aimed to investigate the prevalence of six well-known anatomical variants in the thorax using CT images obtained from an open-access COVID-19 dataset in order to demonstrate the value of public datasets in anatomical research and study the plausible link between anatomical variants and predisposition to COVID-19.

2 | MATERIALS AND METHODS

2.1 | Imaging dataset

The CT images used in the present study were obtained from “COVID19-CT-dataset: an open-access chest CT image repository of

1000+ patients with confirmed COVID-19 diagnosis” (Shakouri et al., 2021), which is available in the Harvard Dataverse.* This dataset consists of unenhanced chest CTs from over 1000 Iranian patients with confirmed COVID-19 diagnosed by positive Reverse Transcription Polymerase Chain Reaction (RT-PCR). The average age was 47.18 ± 16.32 years, and the age range was 6–89 years. The sex distribution was 60.9% male and 39.1% female. The most commonly self-reported coexisting diseases among these patients included hypertension, coronary heart disease, diabetes, and interstitial pneumonia or emphysema. The CT images were obtained between March 2020 and January 2021. All images were in DICOM format with 16-bit grayscale with 512×512 -pixels resolution. Slice thicknesses of the CT scans were in the range of 1.5 or 3.0 millimeters. Patient-specific information was blinded. Ethical approval for this study was exempted by Mahidol University Central Institutional Review Board (MU-CIRB).

2.2 | Image analysis

Six anatomical variants were investigated, including the azygos lobe (AL), tracheal bronchus (TB), cardiac bronchus (CB), sternal foramen (SF), episternal ossicles (EO), and sternalis muscle (SM). The right lung was inspected for an AL by identifying the azygos fissure on axial views. The potential presence of a TB or CB was then evaluated on coronal views. The TB was identified as a supernumerary branching of the trachea above the tracheal bifurcation, while the CB was a short blind-ending bronchial stump pointing towards the mediastinum. All positive findings were then confirmed in axial plane, coronal plane, and 3D view. Subsequently, the sterna of all patients were carefully inspected along the whole length from the jugular notch to the xiphoid process for possible SF, EO, and SM in all three planes. The SF showed a typical “bow-tie” appearance (Duraikannu et al., 2016), while the EO were observed as small ossicles posterior to the superior end of the manubrium in axial view. The SM appeared as a separate muscle belly lying over the pectoralis major parallel to the sternum. The number and location of EO, SF, and SM were recorded. These variants were identified by two observers with consultation from an expert radiologist with 5 years of experience. Any disagreement between the two observers was resolved by the radiologist. Three-dimensional images of the findings were reconstructed on 3D Slicer (Fedorov et al., 2012) using the segmentation editor. The resulting 3D models underwent further editing on Meshlab (Cignoni et al., 2008) and were uploaded to Figshare (Supporting Information S1).

2.3 | Dataset exploration and exclusion

There were 1019 DICOM files in the dataset. Seventeen duplicates were detected and excluded. Twenty-six patients were removed prior to AL identification because the lungs were unclear owing to severe COVID-19 pathology or background noise. Twenty patients were excluded from TB and CB identification because the trachea was not clearly visible. A total of 25 patients was removed from SF

identification because the sternum was unclear owing to background noise, motion artifacts, or sternotomy. Nineteen patients were excluded from EO identification either because the CT was unclear, the superior end of the manubrium was not visible, or sternotomy. Thirty-three patients were excluded from the analysis of the SM because the muscles on the anterior thoracic wall were not clearly visible or distinguishable from the surrounding soft tissue.

3 | RESULTS

The prevalences of the six thoracic anatomical variants are shown in Table 1. The reconstructed 3D images of the anatomical variants are additionally provided in Supporting Information 1.

3.1 | Prevalence of bronchopulmonary variations

The AL was present in eight of 992 patients investigated (0.8%) (Figure 1). In three of these eight cases, the AL was infested with COVID-19. It can clearly be seen that the AL is well separated from the rest of the superior lobe of the right lung by the azygos fissure (Figure 1E), which contains the azygos vein as observed in the coronal plane (Figure 1B and D). Among 999 patients, the TB was present in two (0.2%) (Table 1). It appeared as a well-separated secondary bronchus originating superior to the tracheal bifurcation (Figure 2). In one patient, the TB gave rise to the apical, anterior and posterior bronchopulmonary segments of the superior lobe of the right lung. In the other patient, however, segments of the TB could not be identified due to severe COVID-19 pathology. The CB was not observed in the present study.

3.2 | Prevalence of sternal variations

Of the 994 sternebrae investigated, an SF was present in 95 (9.6%) (Table 1). Among these, it was single in 86 cases (90.5%) (Figure 3) and double in nine (9.5%) (Figure 4). No more than two SFs were present in any patient. The SF could appear at several locations including the sternum, the xiphoid process, or both. The most common type was a single SF in the lower third of the sternum, which accounted for 53.7% (51 cases) of the total. The size and shape of the SF may vary from one individual to another (Figure 4). The second most prevalent (36.8%, 35 cases) was the xiphoidal type in which the SF was present at the xiphoid process. In one case there was a double SF at the xiphoid process (1.0%). In eight cases (8.4%), there were SFs at both the sternal and xiphoid processes in the same patient (Figure 3). No SF was seen at the manubrium.

Incomplete sternal ossification was observed in two patients (0.2%). In one of these, the sternal body was divided into multiple sternebrae (Figure 5). The upper sternebra was only one-third the size of the lower, and the xiphoid process was absent (Figure 5A). In the

TABLE 1 Overall prevalences of anatomical variations observed in COVID-19 chest CT images

Structure and types	Number of observations	Prevalence (%)
<i>Bronchopulmonary variations</i>		
Azygos lobe (AL)	8/992	0.8
Tracheal bronchus (TB)	2/999	0.2
Cardiac bronchus (CB)	0/999	0
<i>Sternal variations</i>		
Sternal foramen (SF)	95/994	9.6
Sternal	51/95	5.1
Xiphoid	35/95	2.5
Double xiphoid	1/95	0.1
Sternal and xiphoid	8/95	0.8
Episternal ossicles (EO)	29/1000	2.9
Left	7/29	0.7
Right	5/29	0.5
Central	2/29	0.2
Sternalis muscle (SM)	15/986	1.5
Left	7/15	0.7
Right	5/15	0.5
Bilateral	4/15	0.4
Type I1	11/15	1.1
Type II1	3/15	0.3
Type II2	1/15	0.1
<i>Other</i>		
Incomplete sternal ossification	2/994	0.2

second case, the sternal body was separated into five sternebrae (Figure 5B). The xiphoid process also appeared unusually flat with no inferior protrusion (Figure 5B). Remarkably, the SF was observed concomitantly with the AL in two cases, accounting for 20% of the total AL cases.

The EO was present in 2.9% (29 patients) of 1000 patients investigated. It appeared as small ossicles in the sternal notch, above the manubrium but inferior to the clavicle (Figure 6). The EO could be either bilateral or unilateral. It was bilateral in 15 patients (51.7%), on the left side only in seven (24.1%), and on the right side only in five (17.2%). In two patients (6.9%), the single EO was located at the center and articulated with the superior border of the manubrium (Figure 6E and F).

Among 986 patients, the SM was present in 15 (1.5%) (Table 1) (Figure 7). The SM was bilateral in only 26.7% (4 cases). It was found on the right or the left side only in 53.3% (eight cases), and 20.0% (three cases), respectively. Based on the classification by Jeleu et al. (2001), 11 cases (1.1%) were identified as type I1. Type II1 and II2 were present in three cases (0.3%) and one case (0.1%), respectively.

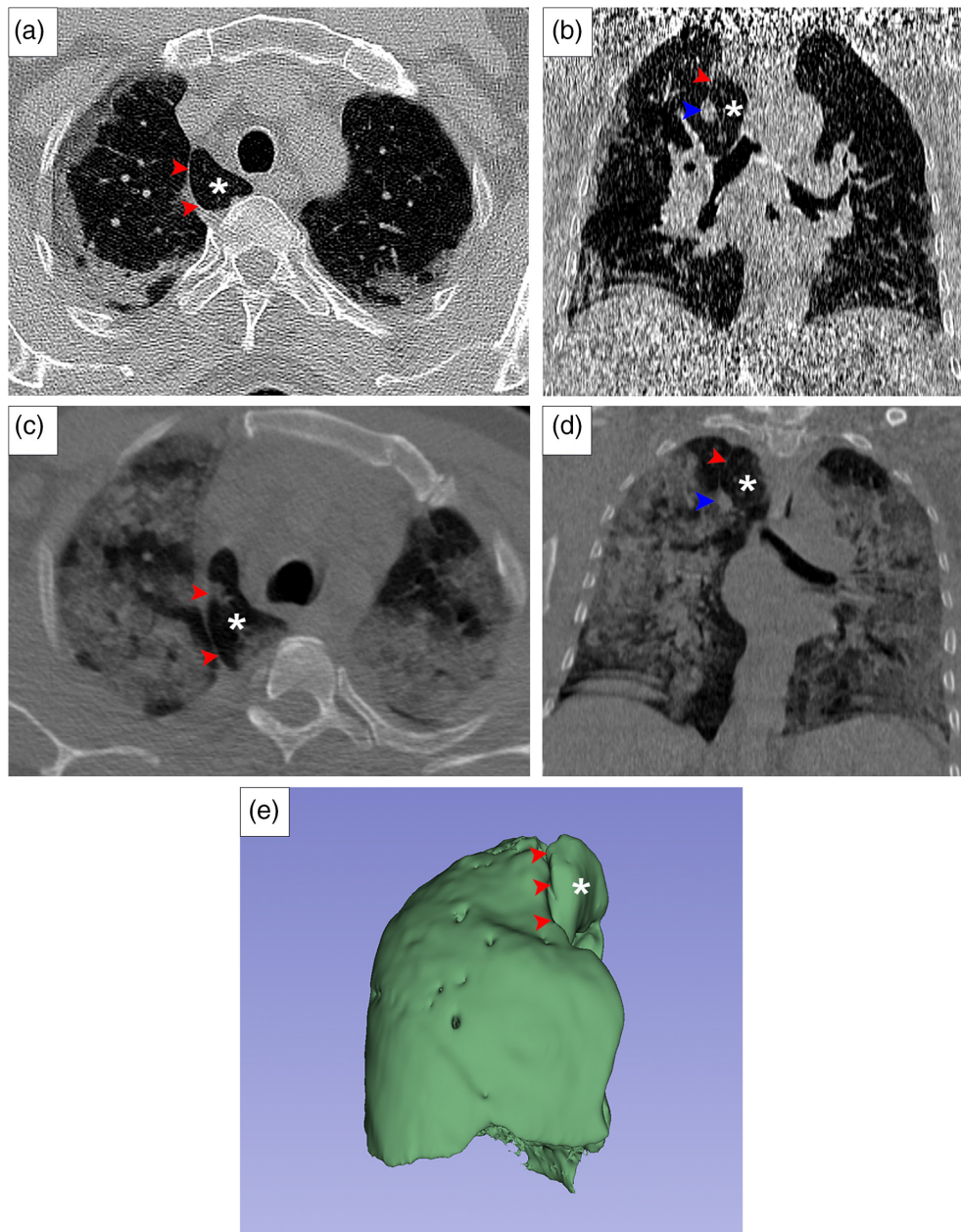


FIGURE 1 Axial (A, C) and coronal (B, D) CT images showing the presence of azygos lobe without (A, B), and with (C, D), COVID-19 pathology. The last panel (E) demonstrates the 3D reconstruction of an AL. The AL is indicated by asterisks. Red arrowheads indicate the azygos fissure while the blue arrowhead indicates the azygos vein. An interactive 3D file is available in the supporting information

4 | DISCUSSION

This is the first anatomical study to be performed using an open-access dataset. Typically, anatomical studies are conducted using institutionally provided materials such as cadaveric samples or dried skeletons provided by donations. In many countries, shortage of body donors results in lower availability of cadavers, which hampers not just dissection opportunities for students but also other cadaver-based activities including anatomical research (Chen et al., 2018; Rajasekhar & Dinesh Kumar, 2021). The COVID-19 pandemic has undoubtedly worsened the situation because of the lack or slow delivery of recommendations from the regulatory authorities regarding the management of donated bodies, causing many institutions to suspend their body donation programs (Rajasekhar & Dinesh Kumar, 2021).

Despite the challenges created by the pandemic, it has opened a window of opportunities for data-driven research. The sharing of large, real-world imaging datasets has been crucial in accelerating COVID-19 research such as automated diagnosis and disease prognosis (Harmon et al., 2020; Shakouri et al., 2021). Apart from COVID-19-related datasets, numerous imaging datasets are available in The Cancer Imaging Archive (TCIA), an open-access information resource to support research, development, and educational initiatives using advanced medical imaging of cancer (Clark et al., 2013). To date, there are 160 imaging datasets in the TCIA from multiple modalities such as CT, magnetic resonance imaging, and ultrasound (The Cancer Imaging Archive, 2022). Re-purposing these datasets for anatomical research has several advantages. Researchers from institutions with no access to medical images can use these datasets for research. Another

FIGURE 2 Coronal (A) and axial (B) CT images showing the tracheal bronchus and its 3D reconstruction (C). The red arrowheads indicate the tracheal bronchus while the blue arrowhead indicates the sternal foramen. An interactive 3D file is available in the supporting information

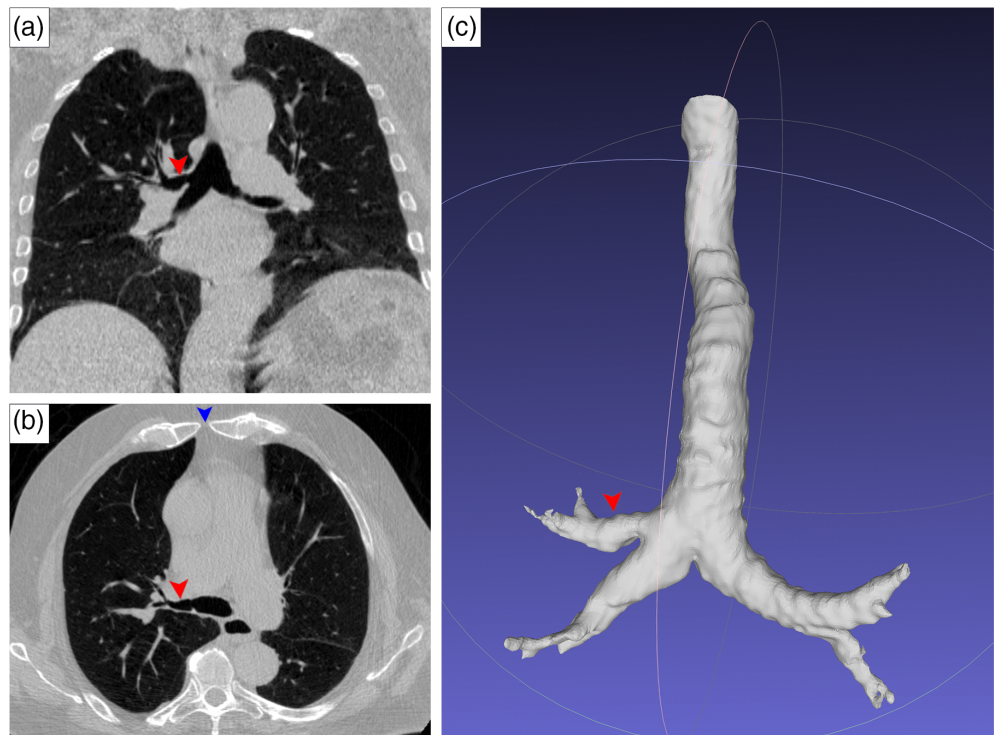
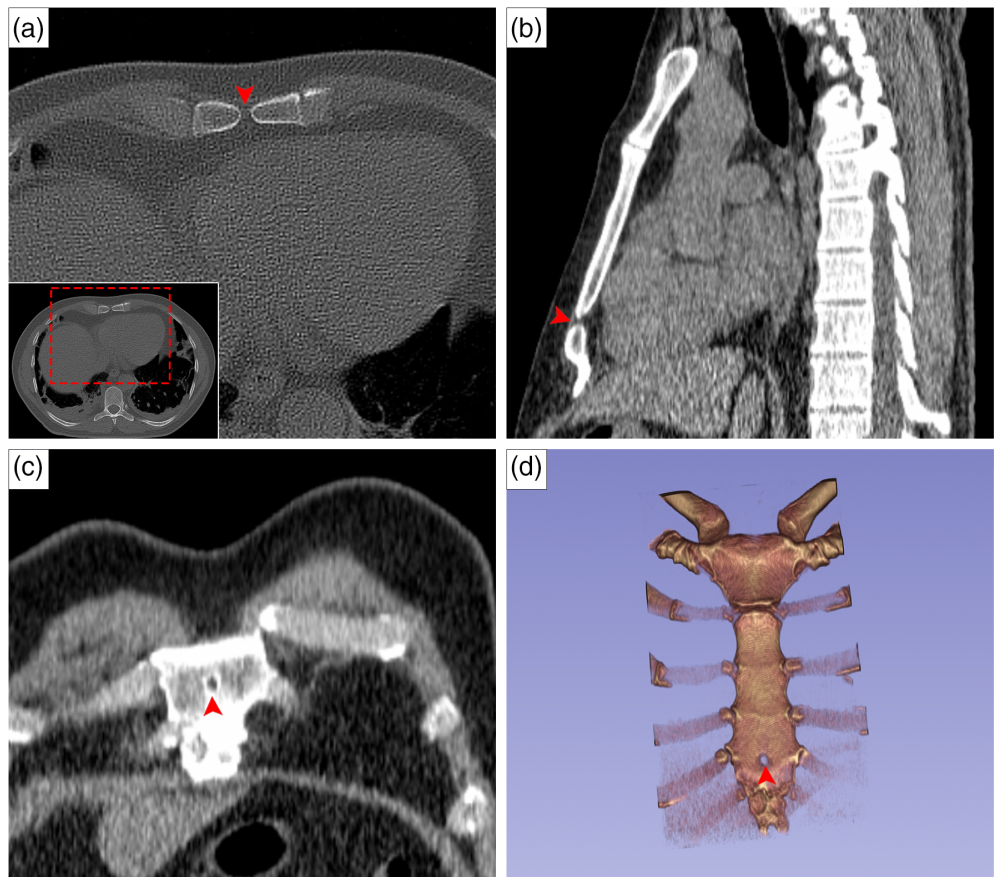


FIGURE 3 Axial (A), sagittal (B), coronal (C) CT images, and 3D reconstruction in anteroposterior view (D) of the sternal foramen (red arrowheads). An interactive 3D file is available in the supporting information



benefit is to uncover possible relationships between variant anatomy and diseases, and any structural changes to normal anatomy induced by disease. The only apparent drawback of using public imaging

datasets is the absence of patient information, making analysis of correlations with age, sex or underlying diseases impossible. While ethical approval is not always necessary because it has been covered by the

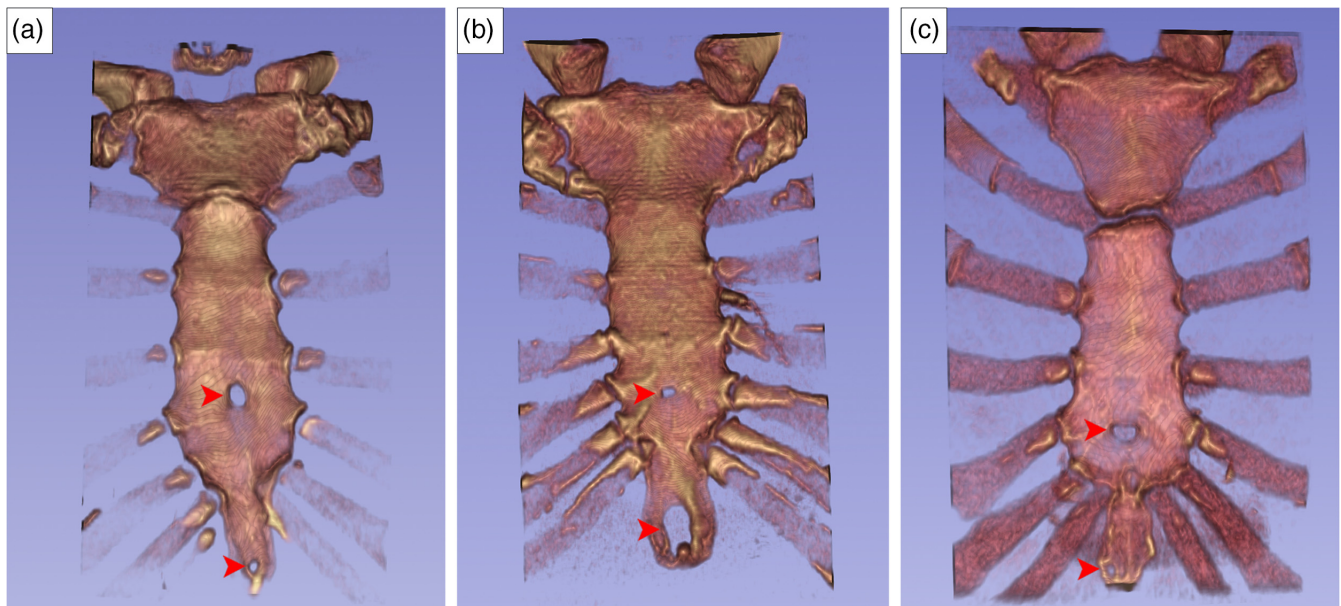


FIGURE 4 Variability in the morphology of the double sternal and xiphoid foramina including relatively equal size (A), unequal size (B) and deviated xiphoid foramen (C). The red arrowheads indicate the sternal and xiphoid foramina

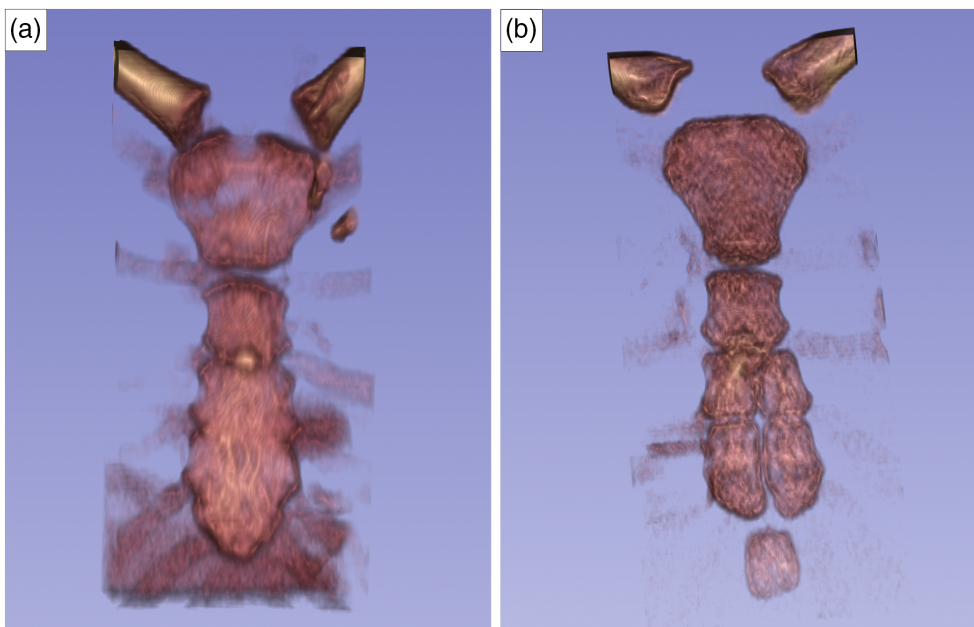


FIGURE 5 Three-dimensional reconstruction from CT images of two patients showing multiple sternbrae accompanied by the absence of xiphoid process (A), and aberrantly flat xiphoid process (B)

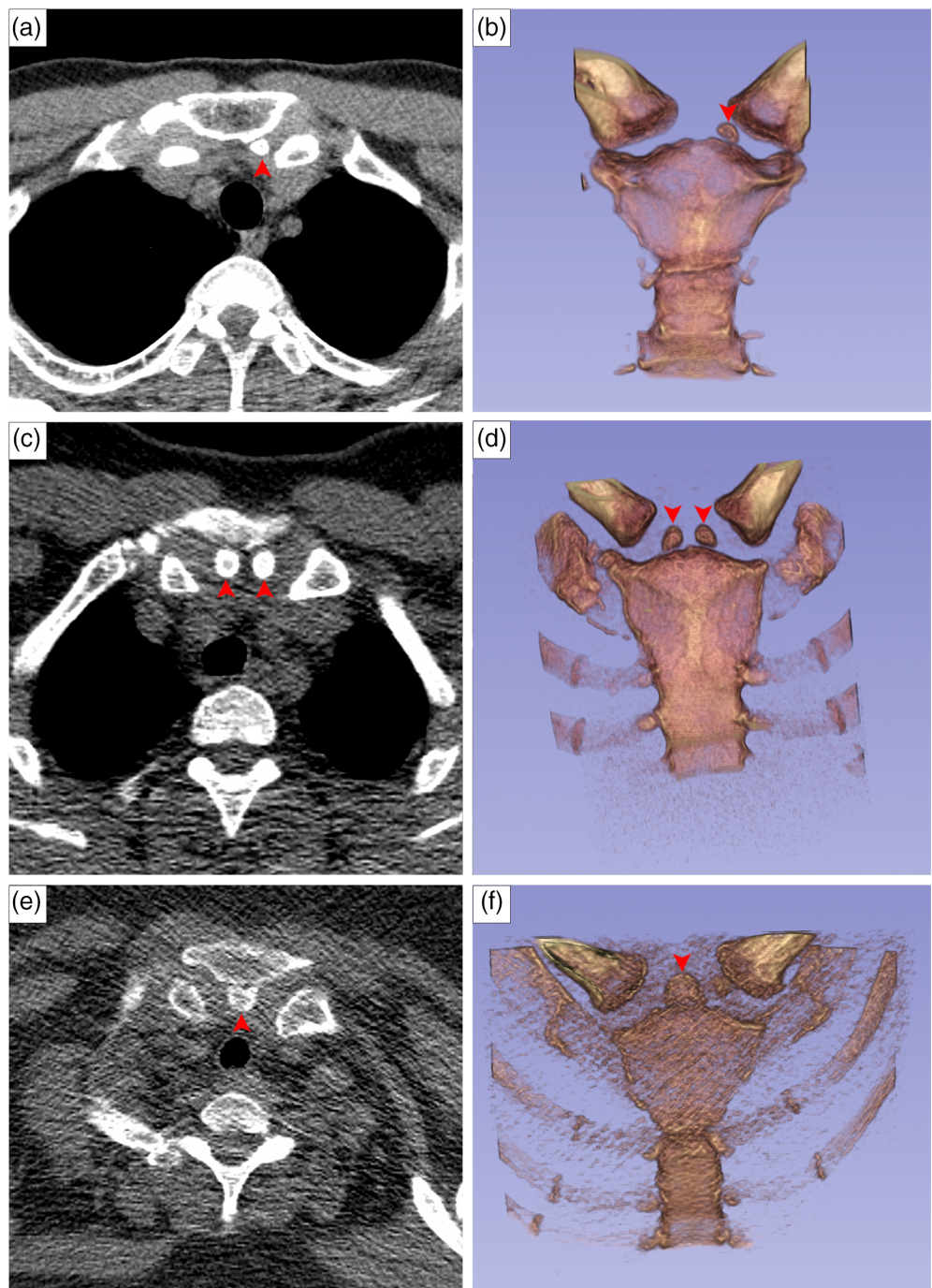
original study, we recommend that researchers consult with their own institution; there could be different arrangements depending on local legal requirements.

In this study, we took advantage of an open-access COVID-19 CT dataset to study the prevalences of six well-known thoracic anatomical variants in the thorax. We found that the AL was present in 0.8% of COVID-19 patients, more than twice the global prevalence (Yurasakpong et al., 2021). However, this finding alone is not sufficient to demonstrate that individuals with an AL are more predisposed to COVID-19 infection than others; the finding could be due to the use of different imaging modalities. In our previous work, we found that most

studies used X-ray to diagnose an AL, and the prevalence of AL obtained from X-ray studies (2.6%) was significantly lower than that from CT studies (6.7%) (Yurasakpong et al., 2021), suggesting that radiographs are less sensitive in detecting the AL. The TB was present in only two patients, a prevalence of 0.2%, which is five times less common than the global average of 1.0% (Wong et al., 2021). The CB was not encountered, possibly because the sample size was insufficient.

The SF is an oval-shaped defect present in 2.5–18.3% of the population (Choi et al., 2017; Kuzucuoglu & Albayrak, 2020). This foramen is typically present in the lower third of the sternal body and the xiphoid process, while an SF at the manubrium is extremely rare

FIGURE 6 Axial CT images (A, C, and E) and 3D reconstruction in anterior view of (B, D, and F) the episternal ossicles including the unilateral (A, B), bilateral (C, D), and central (E, F) types. Red arrowheads indicate the episternal ossicles



(Cooper et al., 1988). In the present study, the prevalence of SF was 9.6%. Moreover, when only those individuals who present with an AL are considered, the prevalence of the SF was twice the population norm (20%; two out of eight cases). Further studies are needed to better understand the co-occurrence of these variations. In addition, incomplete ossification of the sternum was present in two patients, which we believe to be the sternbrae that represent the immature state of the sternum in younger individuals (Bayarogullari et al., 2014).

The SM was observed in only 1.5% in the present study, which is considerably lower than the pooled prevalence of 6% reported in a

recent meta-analysis (Asghar et al., 2022). The authors believe that this marked discrepancy was unrelated to COVID-19 but was due rather to the method used to detect the SM. The SM is typically investigated by cadaveric dissection and multi-detector CT (Asghar et al., 2022). The authors believe that normal CT, as used in the present study, is not as effective as other modalities at exposing subtle differences between the soft tissues. With this reason, it was not possible to distinguish thinner forms of the SM from the surrounding tissues. As a result, we do not recommend further studies using normal CT to study the SM.

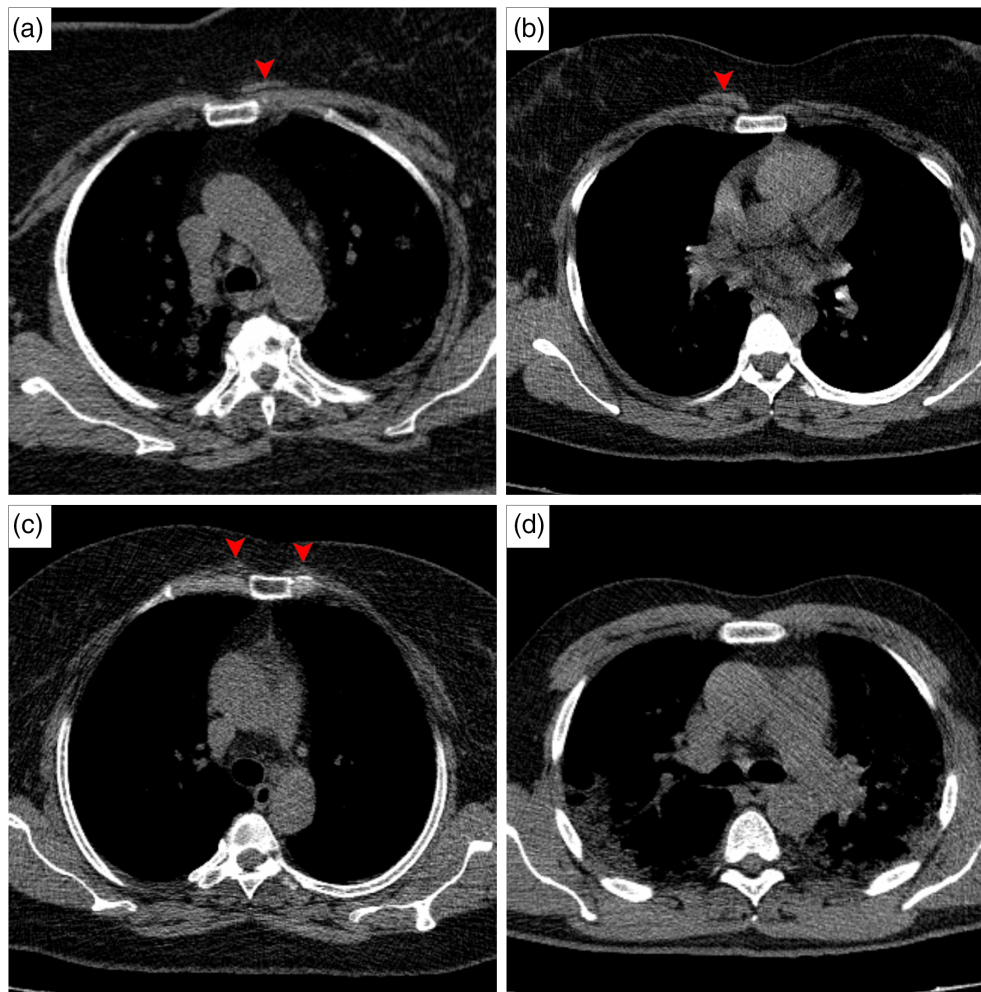


FIGURE 7 Axial CT images showing left side sternalis muscle (a), right-sided sternalis muscle (B), bilateral sternalis muscle (C), and the absence of sternalis muscle (D). Bellies of the sternalis muscle are indicated by red arrowheads

5 | LIMITATIONS

The present study is not without limitations. A few CT images contained background noise and motion artifacts, which led to exclusion. Individual patient details including sex and age were blinded in this dataset, making correlations with factors such as age, sex, weight, and coexisting diseases impossible to analyze. Even though most skeletal variations were investigated, we did not investigate suprasternal tubercles, manubriosternal fusions, sternoxiphoidal fusions, or supernumerary ribs. While the use of open-access data may lead to numerous research opportunities, sampling bias is inevitably introduced. Therefore, further comparative studies are needed to address whether these results are generalizable to the normal population.

6 | CONCLUSION

The present study pilots the feasibility of using open-access datasets in anatomical research by studying the prevalences of six well-known anatomical variants in the thorax using CT images obtained from a publicly available COVID-19 dataset. We believe there is a window of opportunities for applying public imaging datasets in anatomical

research, although further studies are needed to evaluate their potential using more datasets from different body regions as well as other imaging modalities. Awareness and understanding of these anatomical variants are also essential for radiologists when examining chest CTs, especially since their use has accelerated owing to the COVID-19 pandemic.

S1: Links and QR codes of 3D files of the azygos lobe, tracheal bronchus, sternal foramen, and episternal ossicles.

ORCID

Laphatrada Yurasakpong [ID https://orcid.org/0000-0001-6030-8160](https://orcid.org/0000-0001-6030-8160)

Somluk Asuvapongpatana [ID https://orcid.org/0000-0003-1594-6555](https://orcid.org/0000-0003-1594-6555)

Wattana Weerachatanukul [ID https://orcid.org/0000-0002-4365-4800](https://orcid.org/0000-0002-4365-4800)

Krai Meemon [ID https://orcid.org/0000-0001-5700-2646](https://orcid.org/0000-0001-5700-2646)

Nopporn Jongkamonwiwat [ID https://orcid.org/0000-0003-3311-2773](https://orcid.org/0000-0003-3311-2773)

Nutmethee Kruepunga [ID https://orcid.org/0000-0002-3871-1209](https://orcid.org/0000-0002-3871-1209)

Arada Chaiyamon [ID https://orcid.org/0000-0002-4748-9021](https://orcid.org/0000-0002-4748-9021)

Joe Iwanaga [ID https://orcid.org/0000-0002-8502-7952](https://orcid.org/0000-0002-8502-7952)

R. Shane Tubbs [ID https://orcid.org/0000-0003-1317-1047](https://orcid.org/0000-0003-1317-1047)

Athikhun Suwannakhan [ID https://orcid.org/0000-0001-9910-0244](https://orcid.org/0000-0001-9910-0244)

ENDNOTE

* The CT images used in this study was obtained from <https://doi.org/10.7910/DVN/6ACUZI>

REFERENCES

- Afshar, P., Heidarian, S., Enshaei, N., Naderkhani, F., Rafiee, M. J., Oikonomou, A., Fard, F. B., Samimi, K., Plataniotis, K. N., & Mohammadi, A. (2021). COVID-CT-MD, COVID-19 computed tomography scan dataset applicable in machine learning and deep learning. *Scientific Data*, 8, 121.
- Asghar, A., Naaz, S., Narayan, R. K., & Patra, A. (2022). The prevalence and distribution of sternalis muscle: A meta-analysis of published literature of the last two hundred years. *Anatomical Science International*, 97, 110–123.
- Azadbakht, J., Haghi-Aminjan, H., & Farhood, B. (2020). Chest CT findings of COVID-19-infected patients, are there differences between pediatric and adult patients? A systematic review. *Egyptian Journal of Radiology and Nuclear Medicine*, 51, 145.
- Bayarogullari, H., Yengil, E., Davran, R., Aǧlagül, E., Karazincir, S., & Balci, A. (2014). Evaluation of the postnatal development of the sternum and sternal variations using multidetector CT. *Diagnostic and Interventional Radiology*, 20, 82–89.
- Chen, D., Zhang, Q., Deng, J., Cai, Y., Huang, J., Li, F., & Xiong, K. (2018). A shortage of cadavers: The predicament of regional anatomy education in mainland China. *Anatomical Sciences Education*, 11, 397–402.
- Choi, P. J., Iwanaga, J., & Tubbs, R. S. (2017). A comprehensive review of the sternal foramina and its clinical significance. *Cureus*, 9, e1929.
- Cignoni, P., Callieri, M., Corsini, M., Dellepiane, M., Ganovelli, F. and Ranzuglia, G. (2008). Meshlab: An open-source mesh processing tool. Paper presented at the Eurographics Italian Chapter Conference.
- Clark, K., Vendt, B., Smith, K., Freymann, J., Kirby, J., Koppel, P., Moore, S., Phillips, S., Maffitt, D., & Pringle, M. (2013). The cancer imaging archive (TCIA): Maintaining and operating a public information repository. *Journal of Digital Imaging*, 26, 1045–1057.
- Cooper, P. D., Stewart, J. H., & McCormick, W. F. (1988). Development and morphology of the sternal foramen. *The American Journal of Forensic Medicine and Pathology*, 9, 342–347.
- Duraikannu, C., Noronha, O. V., & Sundarajan, P. (2016). MDCT evaluation of sternal variations: Pictorial essay. *Indian Journal of Radiology and Imaging*, 26, 185–194.
- Fedorov, A., Beichel, R., Kalpathy-Cramer, J., Finet, J., Fillion-Robin, J.-C., Pujol, S., Bauer, C., Jennings, D., Fennessy, F., Sonka, M., Buatti, J., Aylward, S., Miller, J. V., Pieper, S., & Kikinis, R. (2012). 3D slicer as an image computing platform for the quantitative imaging network. *Magnetic Resonance Imaging*, 30, 1323–1341.
- Fossey, S., Ather, S., Davies, S., Dhillon, P. S., Malik, N., Phillips, M., & Harden, S. (2021). Impact of COVID-19 on radiology training: Royal College of Radiologists junior radiologists forum national survey. *Clinical Radiology*, 76, 549.e549–549.e515.
- Harmon, S. A., Sanford, T. H., Xu, S., Turkbey, E. B., Roth, H., Xu, Z., Yang, D., Myronenko, A., Anderson, V., & Amalou, A. (2020). Artificial intelligence for the detection of COVID-19 pneumonia on chest CT using multinational datasets. *Nature Communications*, 11, 4080.
- Jelev, L., Georgiev, G., & Surchev, L. (2001). The sternalis muscle in the Bulgarian population: Classification of sternales. *Journal of Anatomy*, 199, 359–363.
- Khatami, F., Saatchi, M., Zadeh, S. S. T., Aghamir, Z. S., Shabestari, A. N., Reis, L. O., & Aghamir, S. M. K. (2020). A meta-analysis of accuracy and sensitivity of chest CT and RT-PCR in COVID-19 diagnosis. *Scientific Reports*, 10, 22402.
- Kuzucuoglu, M., & Albayrak, I. (2020). Topographic evaluation of sternal foramen patients with thoracic computed tomography. *Surgical and Radiologic Anatomy*, 42, 405–409.
- Rajasekhar, S. S. S. N., & Dinesh Kumar, V. (2021). The cadaver conundrum: Sourcing and anatomical embalming of human dead bodies by medical schools during and after COVID-19 pandemic: Review and recommendations. *SN Comprehensive Clinical Medicine*, 3, 924–936.
- Salahshour, F., Mehrabinejad, M.-M., Toosi, M. N., Gity, M., Ghanaati, H., Shakiba, M., Sheybani, S. N., Komaki, H., & Kolahi, S. (2021). Clinical and chest CT features as a predictive tool for COVID-19 clinical progress: Introducing a novel semi-quantitative scoring system. *European Radiology*, 31, 5178–5188.
- Santosh, K., & Ghosh, S. (2021). Covid-19 imaging tools: How big data is big? *Journal of Medical Systems*, 45, 1–8.
- Shakouri, S., Bakhshali, M. A., Layegh, P., Kiani, B., Masoumi, F., Ataei Nakhaei, S., & Mostafavi, S. M. (2021). COVID19-CT-dataset: An open-access chest CT image repository of 1000+ patients with confirmed COVID-19 diagnosis. *BMC Research Notes*, 14, 178.
- Tang, Z., Zhao, W., Xie, X., Zhong, Z., Shi, F., Ma, T., Liu, J., & Shen, D. (2021). Severity assessment of COVID-19 using CT image features and laboratory indices. *Physics in Medicine and Biology*, 66, 035015.
- The Cancer Imaging Archive. (2022). Browse data collection. <https://www.cancerimagingarchive.net/collections/>
- Wang, B., Jin, S., Yan, Q., Xu, H., Luo, C., Wei, L., Zhao, W., Hou, X., Ma, W., & Xu, Z. (2021). AI-assisted CT imaging analysis for COVID-19 screening: Building and deploying a medical AI system. *Applied Soft Computing*, 98, 106897.
- Wong, L. M., Cheruiyot, I., de Oliveira, M. H. S., Keet, K., Tomaszewski, K. A., Walocha, J. A., Tubbs, S., & Henry, B. M. (2021). Congenital anomalies of the tracheobronchial tree: A meta-analysis and clinical considerations. *The Annals of Thoracic Surgery*, 112, 315–325.
- Yurasakpong, L., Yammine, K., Limpanuparb, T., Janta, S., Chaiyamon, A., Kruepunga, N., Meemon, K., & Suwannakhan, A. (2021). The prevalence of the azygos lobe: A meta-analysis of 1,033,083 subjects. *Clinical Anatomy*, 34, 872–883.

SUPPORTING INFORMATION

Additional supporting information may be found in the online version of the article at the publisher's website.

How to cite this article: Yurasakpong, L., Asuvapongpatana, S., Weerachayanukul, W., Meemon, K., Jongkamonwivat, N., Kruepunga, N., Chaiyamon, A., Sudsang, T., Iwanaga, J., Tubbs, R. S., & Suwannakhan, A. (2022). Anatomical variants identified on chest computed tomography of 1000+ COVID-19 patients from an open-access dataset. *Clinical Anatomy*, 35(6), 723–731. <https://doi.org/10.1002/ca.23873>